Antenna Diagnostics on Planar Arrays using a 3D Source Reconstruction Technique and Spherical Near-Field Measurements

Erik Jørgensen*, Doren W. Hess†, Peter Meincke*, Oscar Borries*, Cecilia Cappellin* and Jeff Fordham†

* TICRA
Læderstræde 34, DK-1201 Copenhagen
Denmark
Email: {ej,pme,ob,cc}@ticra.com

†MI Technologies
1125 Satellite Blvd, Suite 100
Suwanee, Georgia 30024, USA
Email: dhess@mi-technologies.com, jfordham@mi-technologies.com

***Abstract*—In this paper, we apply a recently developed 3D source reconstruction algorithm to perform antenna diagnostics on a planar array configuration. The test case is a planar X-band slot array measured in a spherical near-field facility and two slots were intentionally covered during the measurement campaign to test the performance of the algorithm. These measured data have previously been analyzed in [1] using two different methods for planar back-projection. For the purpose of comparison, results obtained with a planar reconstruction method based on conversion of spherical waves are also presented.**

I. Introduction

Antenna Diagnostic procedures on planar arrays are typically performed by back-projection of the measured field onto the antenna aperture. Several techniques have been proposed for this purpose, including Fourier transform based techniques [2], [1] and techniques based on conversion of spherical waves to plane waves (SWE-to-PWE) [3]. These planar reconstruction techniques are computationally inexpensive and may be applied to arbitrarily large planar arrays.

In the last decade, a new class of antenna diagnostics algorithms has been introduced. These new methods are based on discretization of integral equations [4]-[18], e.g., the source reconstruction method (SRM) and the Inverse Method of Moments (INV-MoM). The integral equations are derived by placing unknown equivalent electric and magnetic currents on a surface conformal to the antenna and requiring that the currents radiate the measured field outside the surface and zero field inside the surface. The last requirement is necessary to ensure that the reconstructed currents correspond to the physical fields one would actually measure on the surface of reconstruction [5]. A discrete set of equations are obtained by using a standard Method-of-Moments discretization, e.g., RWG functions on flat triangular facets [15], [16], or higher-order basis functions on curved surfaces [17]. The latter choice has been shown to provide better accuracy and lower memory requirements [18]. A common property of these new methods is that the field can be reconstructed on an arbitrary 3D surface enclosing the antenna, which opens up a range of new applications. The new applications include but is not limited to artificial suppression of currents flowing on a part of the enclosing surface, e.g., a cable or a support structure, as well as pattern enhancement of noisy, truncated, or irregular measurements.

The 3D source reconstruction allows reconstruction surfaces of arbitrary shape and may therefore also be applied to planar arrays, which facilitates a direct comparison between the planar back-propagation techniques and the 3D source reconstruction technique. In this paper, we apply the 3D source reconstruction technique to an 18 inch flat plate slot array operating at X-band. The array was measured in a spherical near-field facility at MI Technologies and also using a large spherical near-field arch. During the measurement campaign, two of the radiating elements were covered with conducting tape for the purpose of testing the antenna diagnostics algorithms. Planar back-projection of the measured field has previously been reported in [1], where two different derivations of the planar back-propagation algorithm were presented. For the purpose of comparison the paper will also report the results obtained with the SWE-to-PWE algorithm of [3].

II. 3D Reconstruction Algorithm

The 3D reconstruction algorithm is based on a higher-order inverse Method of Moments (INV-MoM) [17], [19], and a brief summary is presented below. On the reconstruction surface S enclosing an antenna, the equivalent electric and magnetic

surface current densities are defined as

$$\mathbf{J}_S = \hat{\mathbf{n}} \times \mathbf{H} \tag{1a}$$

$$\mathbf{M}_S = -\hat{\mathbf{n}} \times \mathbf{E}, \tag{1b}$$

where $\hat{\mathbf{n}}$ is the outward normal unit vector, and $\mathbf{E}$ and $\mathbf{H}$ are the fields just outside the surface of reconstruction. These equivalent currents are those corresponding to Love's equivalence principle since they produce zero field inside S. The measured field can be written as

$$\mathbf{E}^{\text{meas}}(\mathbf{r}) = -\eta_0 \mathcal{L}\mathbf{J}_S + \mathcal{K}\mathbf{M}_S \tag{2}$$

where η_0 is the free-space impedance and the integral operators $\mathcal{L}$ and $\mathcal{K}$ are defined as

$$\begin{aligned}\mathcal{L}\mathbf{J}_S = j\omega\mu_0 \Bigg[&\int_S \mathbf{J}_S(\mathbf{r}') G(\mathbf{r}, \mathbf{r}')\, dS' \\ &+ \frac{1}{k_0^2} \int_S \nabla'_S \cdot \mathbf{J}_S(\mathbf{r}') \nabla G(\mathbf{r}, \mathbf{r}')\, dS' \Bigg]\end{aligned} \tag{3a}$$

$$\mathcal{K}\mathbf{M}_S = \int_S \mathbf{M}_S(\mathbf{r}') \times \nabla G(\mathbf{r}, \mathbf{r}')\, dS', \tag{3b}$$

where k_0 is the free-space wavenumber and $G(\mathbf{r}, \mathbf{r}')$ is the scalar Green's function of free space. Equation (2) is referred to as the data equation, since it relates the measured data $\mathbf{E}^{meas}$ and the unknown surface current densities $\mathbf{J}_S$ and $\mathbf{M}_S$. Love's equivalent currents in (1) are only obtained if the field is explicitly forced to zero inside S [5], [16]. This leads to the additional equation

$$-\eta_0 \hat{\mathbf{n}} \times \mathcal{L}\mathbf{J}_S + \left(\hat{\mathbf{n}} \times \mathcal{K} + \frac{1}{2} \right) \mathbf{M}_S = 0, \tag{4a}$$

$$-\left(\hat{\mathbf{n}} \times \mathcal{K} + \frac{1}{2} \right) \mathbf{J}_S - \frac{1}{\eta_0} \hat{\mathbf{n}} \times \mathcal{L}\mathbf{M}_S = 0 \tag{4b}$$

for $\mathbf{r} \in S$. These expressions are referred to as the boundary condition equation.

The surface of reconstruction is discretized using curvilinear patches of up to fourth order. The electric and magnetic surface currents on each patch are expanded as

$$\mathbf{X} = \sum_{m=0}^{M^u} \sum_{n=0}^{M^v - 1} a_{mn}^u \mathbf{B}_{mn}^u + \sum_{m=0}^{M^v} \sum_{n=0}^{M^u - 1} a_{mn}^v \mathbf{B}_{mn}^v \tag{5}$$

where $\mathbf{X} = [\mathbf{J}, \mathbf{M}]$, a_{mn}^u and a_{mn}^v are unknown coefficients, M^u and M^v are the expansion orders along the u- and v-directions, and $\mathbf{B}_{mn}^u$ and $\mathbf{B}_{mn}^v$ are u- and v-directed higher-order Legendre basis functions [20] defined as

$$\mathbf{B}_{mn}^u(u, v) = \frac{\mathbf{a}_u}{\mathcal{J}_s(u, v)} \widetilde{P}_m(u)\, P_n(v)\,, \tag{6a}$$

$$\mathbf{B}_{mn}^v(u, v) = \frac{\mathbf{a}_v}{\mathcal{J}_s(u, v)} \widetilde{P}_m(v)\, P_n(u)\,. \tag{6b}$$

Herein, $\mathbf{a}_u$ and $\mathbf{a}_v$ are the covariant unitary vectors and $\mathcal{J}_s(u, v) = |\mathbf{a}_u \times \mathbf{a}_v|$ is the surface Jacobian. The current expansion above is then inserted in the data equation (2) and the boundary condition equation (4), and appropriate test functions are then introduced in both equations [17]. This leads to the coupled equations

$$\bar{\mathbf{A}}\mathbf{x} \approx \mathbf{b} \text{ and } \bar{\mathbf{L}}\mathbf{x} = \mathbf{0}, \tag{7}$$

where $\mathbf{x}$ is a vector of unknown basis function coefficients, $\mathbf{b}$ contains samples of the measured field, $\bar{\mathbf{A}}$ is a matrix with elements representing the field radiated by a particular basis function observed at the measurement points, and $\bar{\mathbf{L}}$ is a matrix, whose elements represent the field radiated by a particular basis function, weighted by a particular testing function on S. These coupled equations are solved by the iterative solution scheme described in [19], which allows us to achieve an accurate solution by balancing the effects of noise with the requirement of achieving Love's currents. This setup is advantageous compared to merely gathering the matrices $\bar{\mathbf{A}}$ and $\bar{\mathbf{L}}$ to yield the problem

$$\min_{\mathbf{x}} \left\| \begin{bmatrix} \bar{\mathbf{A}} \\ \bar{\mathbf{L}} \end{bmatrix} \mathbf{x} - \begin{bmatrix} \mathbf{b} \\ 0 \end{bmatrix} \right\|_2, \tag{8}$$

as is done elsewhere in the litterature [5], [15], [16], since the stacked matrix cannot adaptively weight the components, thus lacking accuracy as well as the robustness needed to perform well across a range of cases and noise levels.

III. Results

The 3D reconstruction method presented above is applicable to arbitrarily shaped closed surfaces. For the purpose of comparison and cross-validation, the 3D reconstruction algorithm is now applied to a planar array case, which is ideally suited for existing back-projection techniques, e.g., the two methods considered in [1] or the SWE-PWE algorithm of [3]. The array considered here is the linearly polarized X-band flat plate slot array shown in Figure 1. Two slots (shown in red) have been intentionally covered by conducting tape as indicated with the arrows. This array was measured in a spherical near-field facility at MI Technologies and also using a large spherical near-field arch, and the measurements have previously been reported in [1]. The operating frequency of the array is 9.375 MHz, the diameter of the array is 45.7 cm, and the approximate slot spacing is 0.75 wavelengths. The data were recorded on a partial sphere defined by $\theta < 80°$.

The equivalent currents are reconstructed on a box using the 3D reconstruction method outlined in the previous section, which has been implemented in the software package DIATOOL. The top surface of the box is 45.7 cm $\times$ 45.7 cm and coincides with the array aperture. The box is 2.0 cm deep and a zero-field boundary condition is imposed on the back, thus forcing both the equivalent electric and magnetic currents to zero. The box is discretized using 510 patches with an approximate side length of one wavelength and the total number of unknowns is 17,040. The amplitude and phase of the co-polar tangential electric field are shown in Figure 2 where the locations of the two covered slots are clearly seen. In the region surrounding the slots, the amplitude distribution exhibits a significant dip and the phase pattern shows a distinct

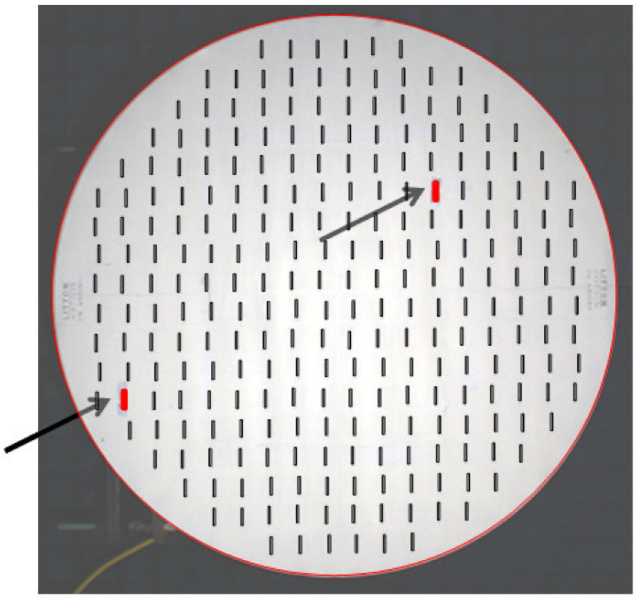

Fig. 1. X-band flat plate array. Two slots have been covered with conducting tape, as indicated by the arrows.

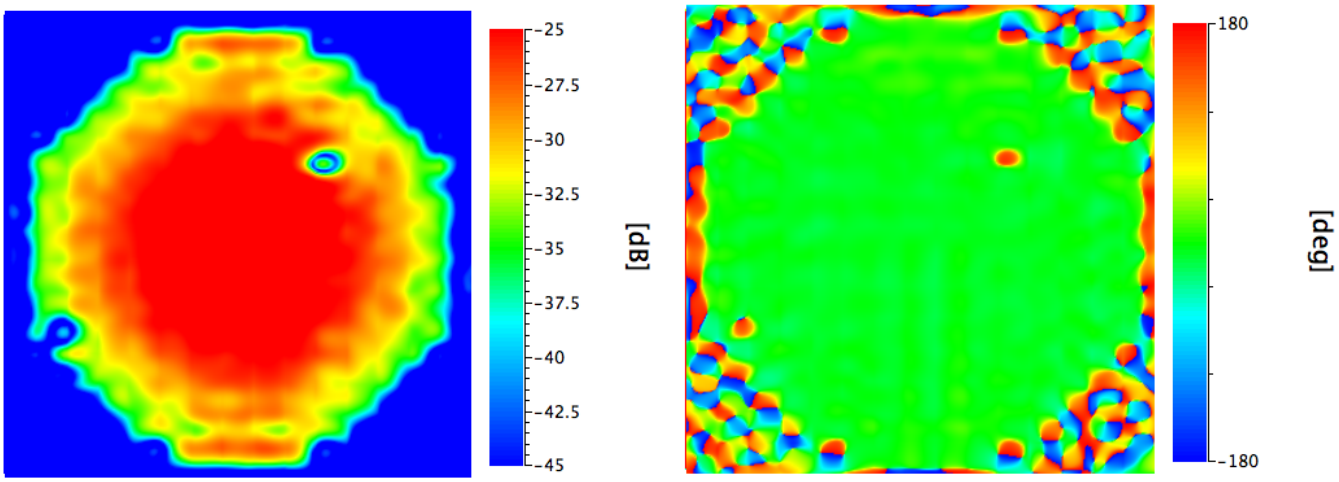

Fig. 2. Reconstructed co-polar field obtained with the 3D reconstruction method (INV-MoM). The field is reconstructed on a box. The plots show the field on the top surface of the box, coinciding with the array aperture. Left: Amplitude. Right: Phase.

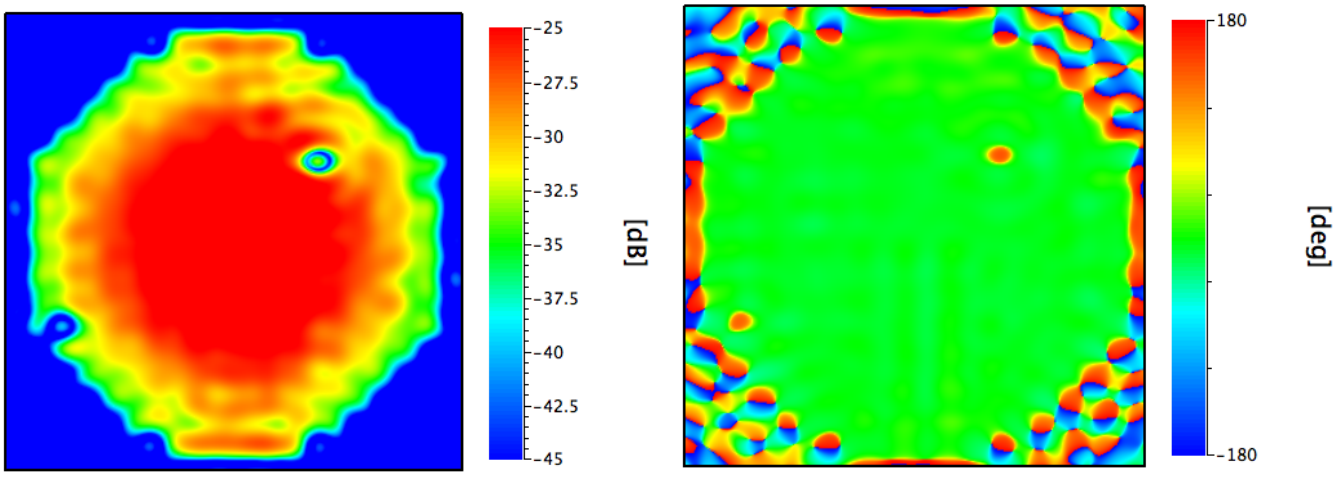

Fig. 3. Reconstructed co-polar field obtained with the planar reconstruction method (SWE-PWE). The field is reconstructed on the array aperture. Left: Amplitude. Right: Phase.

180 degree phase shift allowing a very easy identification of the affected slots.

The SWE-PWE conversion method of [3] can also be applied to the flat plate array considered above. The method in principle allows evanescent waves to be included in the back-projection but for the example considered here convergence is only achieved in the visible region. The results are shown in Figure 3 where the covered slots can easily be detected.

The reconstructed aperture fields shown in Figures 2 and 3, as well as the results reported in [1], all agree very well. For the present test case, it therefore appears that the 3D source reconstruction method [17], the SWE-PWE method, and the back-projection methods in [1] are all capable of extracting the full information embedded in the measured field. However, for smaller arrays the 3D source reconstruction method provides higher accuracy than the planar reconstruction method, which allows identification of the individual array elements in the reconstructed aperture field.

IV. Conclusions

We have applied a recently developed 3D source reconstruction algorithm to reconstruct the aperture field of a flat plate slot array operating at X-band. The reconstructed aperture field was essentially identical to the aperture field obtained by a SWE-PWE conversion procedure, and compared very well to the back-projected aperture fields reported in [1]. The investigations presented in this paper show that both planar back-projection and 3D source reconstruction are viable techniques for performing antenna diagnostics on planar apertures. The back-projection algorithms are superior in terms of memory and CPU time but the 3D source reconstruction technique provides higher accuracy on smaller arrays, which will be demonstrated by numerical examples at the conference. In addition, the 3D source reconstruction is applicable to non-planar geometries and surfaces conformal to the antenna. This latter property opens up a range of new applications, e.g., filtering of undesired currents flowing on cables or support structures.

References

[1] D. Hess and S. McBride, "An aperture back-projection technique and measurements made on a flat plate array with a spherical near-field arch," *Antennas & Propagation Conference, 2009. LAPC 2009. Loughborough*, pp. 733 – 736, 2009.

[2] A. C. Newell, B. Schluper, and R. Davis, "Holographic projection to an arbitrary plane from spherical near-field measurements," *2001 Symposium Digest of the Antenna Measurement Technigues Association*, pp. 92–97, 2001.

[3] C. Cappellin,O. Breinbjerg, A. Frandsen, "Properties of the transformation from the spherical wave expansion to the plane wave expansion," *Radio Science*, vol. 43, no. RS1012, doi:10.1029/2007RS003696, February 2008.

[4] T. K. Sarkar and A. Taaghol, "Near-field to near/far-field transformation for arbitrary near-field geometry utilizing and equivalent electric current and MoM," *IEEE Trans. Antennas Propagat.*, vol. 47, no. 3, pp. 566–573, Mar. 1999.

[5] K. Persson and M. Gustafsson, "Reconstruction of equivalent currents using a near-field data transformation - with radome applications," *Progress in Electromagnetics Research*, vol. 54, pp. 179–198, 2005.

[6] F. Las-Heras and T. K. Sarkar, "Evaluating near-field radiation patterns of commercial antennas," *IEEE Trans. Antennas Propagat.*, vol. 54, no. 8, pp. 2198–2207, Aug. 2006.

[7] Y. Alvarez, F. Las-Heras, and M. R. Pino, "Reconstruction of equivalent currents distribution over arbitrary three-dimensional surfaces based on integral equation algorithms," *IEEE Trans. Antennas Propagat.*, vol. 55, no. 12, pp. 3460–3468, Dec. 2007.

[8] Y. Alvarez, S. T, K, and F. Las-Heras, "Improvement of the sources reconstruction techniques: Analysis of the svd algorithm and the rwg basis functions," in *IEEE Antennas and Propagation Society International Symposium*, Honolulu, Hawaii, USA, July 2007.

[9] Y. Alvarez, F. Las-Heras, M. R. Pino, and J. A. Lopez, "Acceleration of the sources reconstruction method via the fast multipole technique," in *IEEE Antennas and Propagation Society International Symposium*, San Diego, CA, USA, July 2008.

[10] F. Mioc, J. A. Quijano, G. Vecchi, E. Martini, F. Milani, R. Guidi, L. J. Foged, and M. Sabbadini, "Source modelling and pattern enhancement for antenna farm analysis," in *30th ESA Antenna Workshop on Antennas for Earth Observation, Science, Telecommunication and Navigation Space Missions*, Noordwijk, The Netherlands, May 2008, pp. 555–559.

[11] T. F. Eibert and C. H. Schmidt, "Multilevel fast multipole accelerated inverse equivalent current method employing rao-wilton-glisson discretization of electric and magnetic surface currents," *IEEE Trans. on Antennas Propag.*, vol. 57, no. 4, pp. 1178–1185, 2009.

[12] Y. A. Lopez, F. L.-H. Andres, M. R. Pino, and T. K. Sarkar, "An improved super-resolution source reconstruction method," *IEEE Trans. Instrumentation and Measurement*, vol. 58, no. 11, pp. 3855–3866, Nov. 2009.

[13] C. H. Schmidt, Ismatullah, and T. F. Eibert, "Comparison of lower and higher order basis functions in inverse equivalent current methods," *Applied Computational Electromagnetics Society (ACES) Conference, Tampere, Finland*, April 2010.

[14] Y. Alvarez, F. Las-Heras, and M. R. Pino, "Antenna characterization using the sources reconstruction method," in *EuCAP Proceedings*, Barcelona, Spain, April 2010.

[15] J. L. A. Quijano and G. Vecchi, "Improved-accuracy source reconstruction on arbitrary 3-D surfaces," *IEEE Antennas and Wireless Propagation Letters*, vol. 8, pp. 1046–1049, 2009.

[16] ——, "Field and source equivalence in source reconstruction on 3D surfaces," *Progress in Electromagnetics Research*, vol. PIER-103, pp. 67–100, 2010.

[17] E. Jørgensen, P. Meincke, C. Cappellin, and M. Sabbadini, "Improved source reconstruction technique for antenna diagnostics,," in *Proceeedings of the 32nd ESA Antenna Workshop*, ESTEC, Noordwijk, The Netherlands, 2010.

[18] E. Jørgensen, P. Meincke, O. Borries, and M. Sabbadini, "Processing of measured fields using advanced inverse method of moments algorithm,," in *Proceeedings of the 33rd ESA Antenna Workshop*, ESTEC, Noordwijk, The Netherlands, 2011.

[19] ——, "Processing of measured fields using advanced inverse method of moments algorithm," *Proceedings of the 33rd ESA Antenna Workshop, ESTEC, Noordwijk, The Netherlands*, 2010.

[20] E. Jørgensen, J. L. Volakis, P. Meincke, and O. Breinbjerg, "Higher order hierarchical Legendre basis functions for electromagnetic modeling," *IEEE Transactions on Antennas and Propagation*, vol. 52, no. 11, pp. 2985–2995, Nov. 2004.